J|A|C|S
ARTICLES

Published on Web 08/12/2009

Identification of the Structural Phases of $Ce_xZr_{1-x}O_2$ by Eu(III) Luminescence Studies

Tiziano Montini,[†] Adolfo Speghini,*[,‡] Loredana De Rogatis,[†] Barbara Lorenzut,[†] Marco Bettinelli,[§] Mauro Graziani,[†] and Paolo Fornasiero*[,†]

Chemistry Department, ICCOM-CNR, INSTM, Center of Excellence for Nanostructured Materials (CENMAT), University of Trieste, via L. Giorgieri 1, 34127 Trieste, Italy, DiSTeMeV and INSTM, University of Verona, Via della Pieve 70, 37029 San Floriano, Verona, Italy, and Laboratory of Solid State Chemistry, Department of Biotechnology, INSTM, University of Verona, Strada Le Grazie 15, 37128 Verona, Italy

Received June 23, 2009; E-mail: pfornasiero@units.it; adolfo.speghini@univr.it

Abstract: Despite the wide application of ceria-zirconia based materials in Three Way Catalysts (TWCs), Solid Oxides Fuel Cells (SOFCs), and H_2 production and purification reactions, an active debate is still open on the correlation between their structure and redox/catalytic performances. Existing reports support the need of either (i) a homogeneous solid solution or (ii) materials with nanoscale heterogeneity to obtain high activity and stability. Here we report on a simple and inexpensive approach to solve this problem taking advantage of the luminescence properties of Eu(III), used as a structural probe introduced either in the bulk or on the surface of the samples. In this way, the real structure of ceria-zirconia materials can be revealed even for amorphous high surface area samples. Formation of small domains is observed in catalytically important metastable samples which appear homogeneous by conventional XRD.

Introduction

Ceria (CeO_2) based systems are extensively investigated due to their wide applications in materials science. In fact ceria is able to easily form oxygen vacancies releasing surface and lattice oxygen.[1] Due to the high mobility of their lattice oxygen ions, CeO_2-based materials are widely used as promoters in Three Way Catalysts (TWCs)[2] and appear to be promising as active supports/cocatalysts for reforming[3,4] and hydrogen purification reactions,[5,6] as well as electrolyte or electrode promoters in SOFC fabrication.[7,8] Doped with Zr(IV), CeO_2 acquires a particular thermal stability and excellent redox properties, forcing enormous and still growing attention to these materials.

$Ce_xZr_{1-x}O_2$ solid solutions can be prepared with particular attention to their morphology, to maximize their performance as catalyst supports.[9,10] $Ce_xZr_{1-x}O_2$ can exist in three stable phases (monoclinic (m), tetragonal (t), cubic (c)) and in various metastable phases (t', t'', κ, and t^*) depending on the composition and preparation conditions.[11−14] Oxygen deficient structures, such as pyrochlore, may also be formed (either in the bulk[13,15] or as nuclei on the surface[16,17]), and they have been related with the low reduction temperature of $Ce_xZr_{1-x}O_2$.[18] Due to the complexity of the phase diagram, a great effort has been devoted to verify the phase homogeneity of these materials. Conventional techniques, such as XRD and Raman spectroscopy, fail in the investigation of the samples with low crystallinity which, however, are of major interest in catalysis. More complex techniques, such as neutron diffraction, proved to be able to identify inhomogeneities even in the samples that appear

[†] University of Trieste.
[‡] DiSTeMeV, University of Verona.
[§] Laboratory of Solid State Chemistry, University of Verona.

(1) Esch, F.; Fabris, S.; Zhou, L.; Montini, T.; Africh, C.; Fornasiero, P.; Comelli, G.; Rosei, R. *Science* **2005**, *309* (5735), 752–755.
(2) Kaspar, J.; Fornasiero, P.; Graziani, M. *Catal. Today* **1999**, *50* (2), 285–298.
(3) Deluga, G. A.; Salge, J. R.; Schmidt, L. D.; Verykios, X. E. *Science* **2004**, *303* (5660), 993–997.
(4) Salge, J. R.; Dreyer, B. J.; Dauenhauer, P. J.; Schmidt, L. D. *Science* **2006**, *314* (5800), 801–804.
(5) Ratnasamy, P.; Srinivas, D.; Satyanarayana, C. V. V.; Manikandan, P.; Kumaran, R. S. S.; Sachin, M.; Shetti, V. N. *J. Catal.* **2004**, *221* (2), 455–465.
(6) Ruettinger, W.; Liu, X. S.; Farrauto, R. J. *Appl. Catal., B* **2006**, *65* (1−2), 135–141.
(7) McIntosh, S.; Gorte, R. J. *Chem. Rev.* **2004**, *104* (10), 4845–4865.
(8) Steele, B. C. H. *Nature* **1999**, *400* (6745), 619–621.
(9) Liang, X.; Wang, X.; Zhuang, Y.; Xu, B.; Kuang, S.; Li, Y. *J. Am. Chem. Soc.* **2008**, *130* (9), 2736–2737.
(10) Yuan, Q.; Liu, Q.; Song, W. G.; Feng, W.; Pu, W. L.; Sun, L. D.; Zhang, Y. W.; Yan, C. H. *J. Am. Chem. Soc.* **2007**, *129* (21), 6698–6699.
(11) Yashima, M.; Arashi, H.; Kakihana, M.; Yoshimura, M. *J. Am. Ceram. Soc.* **1994**, *77* (4), 1067–1071.
(12) Yashima, M.; Hirose, T.; Katano, S.; Suzuki, Y.; Kakihana, M.; Yoshimura, M. *Phys. Rev. B* **1995**, *51* (13), 8018–8025.
(13) Omata, T.; Kishimoto, H.; Otsuka-Yao-Matsuo, S.; Ohtori, N.; Umesaki, N. *J. Solid State Chem.* **1999**, *147* (2), 573–583.
(14) Kishimoto, H.; Omata, T.; Otsuka-Yao-Matsuo, S.; Ueda, K.; Hosono, H.; Kawazoe, H. *J. Alloys Compd.* **2000**, *312* (1−2), 94–103.
(15) Thomson, J. B.; Armstrong, A. R.; Bruce, P. G. *J. Am. Chem. Soc.* **1996**, *118* (45), 11129–11133.
(16) Montini, T.; Banares, M. A.; Hickey, N.; Di Monte, R.; Fornasiero, P.; Kaspar, J.; Graziani, M. *Phys. Chem. Chem. Phys.* **2004**, *6* (1), 1–3.
(17) Perez-Omil, J. A.; Bernal, S.; Calvino, J. J.; Hernandez, J. C.; Mira, C.; Rodriguez-Luque, M. P.; Erni, R.; Browning, N. D. *Chem. Mater.* **2005**, *17* (17), 4282–4285.
(18) Montini, T.; Hickey, N.; Fornasiero, P.; Graziani, M.; Banares, M. A.; Martinez-Huerta, M. V.; Alessandri, I.; Depero, L. E. *Chem. Mater.* **2005**, *17* (5), 1157–1166.

homogeneous from XRD analysis,[19] revealing the presence of nanometric domains with different compositions. In this work, we demonstrate the potential of luminescence spectroscopy to investigate the homogeneity of $Ce_xZr_{1-x}O_2$ material, using the Eu(III) ion as a structural probe. This technique can provide a detailed picture of the local environment of the cations in these materials, since the luminescence properties of Eu(III) are strongly influenced by the local environment around the lanthanide ion.[20−22]

The structural characteristics of $Ce_xZr_{1-x-0.01}Eu_{0.01}O_{2-\delta}$ materials ($x = 0.20$, 0.50, and 0.80) were analyzed as a function of the calcination temperature. To this purpose, the materials were doped with a relatively low concentration of Eu(III) ions (1 mol %) with the purpose of using it as a structural probe entering the Ce(IV) and Zr(IV) sites,[20−22] without appreciably altering structural properties and catalytic activities. They will be denoted as CZE-X, where X is the molar fraction of Ce(IV), and were doped with Eu(III) either in the bulk or selectively on the surface. All the samples were characterized in terms of BET surface area, powder XRD, Raman spectroscopy, and Eu(III) luminescence spectroscopy, evidencing the possibility of the use of this simple technique to reveal even a small amount of inhomogeneity in $Ce_xZr_{1-x}O_2$ materials.

Experimental Section

Preparation of the Materials. $Ce(NO_3)_3 \cdot 6H_2O$ (99.999% REactron, Alfa Aesar), $ZrO(NO_3)_2 \cdot xH_2O$ (99.99%, Aldrich), and $Eu(NO_3)_3 \cdot 5H_2O$ (99.9%, Aldrich) were used as metal precursors. High purity precursors of Ce and Zr were used to avoid contamination by other rare earths, the presence of which leads to the presence of an f−f transition complicating the interpretation of the Raman spectra of the ceria-zirconia materials.[23]

Bulk-doped samples were prepared as follows: an aqueous solution of the metal precursors was added dropwise to a 10% NH_4OH aqueous solution under vigorous stirring. After complete cation precipitation, H_2O_2 was added to oxidize $Ce(OH)_3$ to $Ce(OH)_3(O_2H)$ and to stabilize the textural network of the material.[24] The solid was then suspended in 2-propanol and refluxed for 5 h to remove water from the gel.[25] Finally, the solid was filtered, dried at 393 K for a day, and calcined in air at 773 K for 5 h.

For the preparation of the surface-doped samples, the same procedure described above was adopted, with the only exception that the Eu salt was not used. After calcination following the desired procedure (temperature and time), the material was impregnated with an aqueous solution of Eu(III) nitrate, dried at 393 K, and calcined at 773 K for an additional 5 h.

Physical Characterization. X-ray powder diffraction spectra were collected using a Philips X'Pert instrument with Cu Kα radiation. The $K_{\alpha 2}$ contribution was subtracted. The cell parameters of each sample have been obtained by fitting the XRD spectra using the PowderCell 2.4 software. The mean crystallite size was calculated applying the Scherrer formula to the principal reflection of the spectra.

Surface area and pore distribution of the samples were obtained by N_2 physisorption at liquid nitrogen temperature using an ASAP 2020 Micromeritics instrument, after degassing the sample at 623 K for 18 h.

Raman spectra of the samples were collected in the anti-Stokes range of 100−3500 cm^{-1} using a Perkin-Elmer 2000 FT-Raman spectrometer. The samples have been excited using a diode-pump Nd:YAG laser (excitation wavelength 1064 nm).

Luminescence Studies. The second harmonic radiation (at 532.0 nm) of a Nd:YAG laser or the 488.0 nm line of an argon laser were used to excite the luminescence spectra. The signal was collected using an optical fiber and dispersed with a 0.46 m monochromator equipped with 150 lines/mm (for the 550−750 nm wavelength range) and 1200 lines/mm (for the 576−582 nm wavelength range) gratings. The signal was then detected with an air cooled CCD device. All the spectroscopic measurements were performed at room temperature.

Results and Discussion

Analysis of $Ce_xZr_{1-x}O_2$ with Thermodynamically Stable Composition. Two homogeneous $Ce_xZr_{1-x}O_2$ materials with thermodynamically stable composition were chosen from the phase diagram[11−14] to investigate the differences in the Eu(III) luminescence induced by the different crystal structures of the host material: a Zr-rich material (CZE-20) and a Ce-rich material (CZE-80).

Table 1 summarizes the main textural and structural features of the CZE-20 and CZE-80 samples obtained from N_2 physisorption and Rietveld analysis of the XRD patterns, respectively. The materials calcined at low temperature (773 K) present high surface areas and appear homogeneous at the XRD scale (see Supporting Information, Figures S1 and S2). The materials with $x = 0.20$ and 0.80 can be identified as of t' and c phases, respectively, by Raman spectroscopy (see Supporting Information, Figures S3 and S4).[11]

After treatment at high temperature, a strong sinterization of all the materials was observed. In accordance with the phase diagram, the bulk-doped CZE-20 is still homogeneous even after treatment at a very high temperature (1673 K). Similar is the situation of the CZE-80 sample, although in this case the material is treated at a lower temperature (1273 K). Raman spectroscopy confirms the homogeneity observed by XRD: the Raman bands are sharper and a small blue shift is observed after high temperature treatment, as a result of the crystallites growth.[26]

The room temperature luminescence spectra of the tetragonal CZE-20 samples are dominated by intense bands assigned to the electric dipole $^5D_0 \rightarrow {}^7F_2$ transition (see Supporting Information, Figures S5), irrespective of the presence of Eu(III) in the bulk or on the surface. This transition is hypersensitive and therefore especially affected by the local site symmetry.[27] Figure 1 shows in detail the electric dipole $^5D_0 \rightarrow {}^7F_0$ transition (denoted in the following as 0−0 transition) which relates to nondegenerate levels ($J = 0$) that are therefore not split by the crystal field interaction,[21] and as such, the spectral features assigned to this transition allow the number of sites accommodating nonequivalent Eu(III) ions to be obtained. In the CZE-20 samples, the band due to this transition is very weak with respect to the other $^5D_0 \rightarrow {}^7F_J$ ($J = 1, 2$) bands. In fact, the 0−0 transition intensity is strongly affected by the site symmetry, and the regular cationic sites in the tetragonal phase of CZE-20 have a

(19) Mamontov, E.; Brezny, R.; Koranne, M.; Egami, T. *J. Phys. Chem. B* **2003**, *107* (47), 13007–13014.
(20) Reisfeld, R.; Zigansky, E.; Gaft, M. *Mol. Phys.* **2004**, *102* (11−12), 1319–1330.
(21) Bunzli, J. C. G.; Choppin, G. R. *Lanthanide Probes in Life, Chemical and Earth Sciences - Theory and Practice*; Elsevier: Amsterdam, 1989.
(22) Capobianco, J. A.; Proulx, P. P.; Raspa, N. *Chem. Phys. Lett.* **1989**, *161* (2), 151–157.
(23) Fornasiero, P.; Speghini, A.; Di Monte, R.; Bettinelli, M.; Kaspar, J.; Bigotto, A.; Sergo, V.; Graziani, M. *Chem. Mater.* **2004**, *16* (10), 1938–1944.
(24) Lee, J. S.; Choi, S. C. *Mater. Lett.* **2004**, *58* (3−4), 390–393.
(25) Jones, S. L.; Norman, C. *J. Am. Ceram. Soc.* **1988**, *71* (4), C190–C191.
(26) Weber, W. H.; Hass, K. C.; McBride, J. R. *Phys. Rev. B* **1993**, *48* (1), 178–185.
(27) Peacock, R. D. *Struct. Bonding (Berlin)* **1975**, *22*, 83–122.

Table 1. Physical Characteristics of the Thermodynamically Stable CZE-80 and CZE-20 Materials after Various Thermal Treatments

sample	treatment	BET surface area ($m^2\ g^{-1}$)	phase (wt%)	a [a] (nm)	c [a] (nm)	c/a	crystallite size[b] (nm)
bulk-doped CZE-20	773 K, 5 h	128	t' ($P4_2nmc$) (100%)	0.5163	0.5246	1.016	7
	1273 K, 5 h	42	t' ($P4_2nmc$) (100%)	0.5165	0.5251	1.016	19
	1673 K, 5 h	<2	t' ($P4_2nmc$) (100%)	0.5146	0.5233	1.017	55
surface-doped CZE-20	773 K, 5 h	111	t' ($P4_2nmc$) (100%)	0.5173	0.5235	1.012	8
bulk-doped CZE-80	773 K, 5 h	170	c ($Fm\bar{3}m$) (100%)	0.5367	---	1	5
	1273 K, 5 h	24	c ($Fm\bar{3}m$) (100%)	0.5367	---	1	25
surface-doped CZE-80	773 K, 5 h	134	c ($Fm\bar{3}m$) (100%)	0.5360	---	1	6
	1273 K, 5 h	15	c ($Fm\bar{3}m$) (100%)	0.5365	---	1	27

[a] Values for the pseudocubic unit cell. [b] Calculated applying the Scherrer formula to the (101) reflection of the tetragonal phase or to the (111) reflection of the cubic phase.

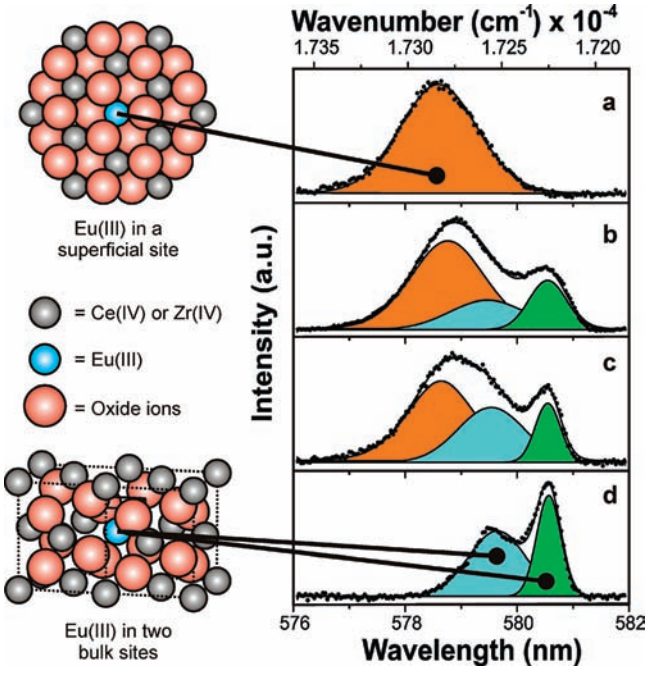

Figure 1. Eu(III) emission spectra of the thermodynamically stable tetragonal CZE-20 samples with the schematic representation of the Eu surface site located on the stable (101) surface of tetragonal $Ce_{0.2}Zr_{0.8}O_2$ and of the two Eu bulk sites of $Ce_{0.2}Zr_{0.8}O_2$ as indicated by EXAFS data.[29] The details of the $^5D_0 \rightarrow {}^7F_0$ transition are reported for both surface and bulk Eu(III) doped materials after different thermal treatments: (a) surface-doped CZE-20 calcined at 773 K for 5 h, (b) bulk-doped CZE-20 calcined at 773 K for 5 h, (c) bulk-doped CZE-20 calcined at 1273 K for 5 h, (d) bulk-doped CZE-20 calcined at 1673 K for 5 h. In accordance with XRD pattern and Raman spectra, all materials show Eu(III) emission spectra consistent with the presence of a single tetragonal t' phase.

D_{2d} site symmetry, for which the $^5D_0 \rightarrow {}^7F_0$ transition of Eu(III) is forbidden.[27] Nevertheless, it can be observed due to small distortions of the Eu(III) sites caused by defects due to charge compensation, as in the case of Eu(III) as a dopant in tetragonal ZrO_2,[28] isostructural to tetragonal CZE-20. Charge compensation occurs also for the other CZE materials discussed below. The 576−582 nm spectral region for the surface-doped CZE-20 calcined at 773 K (Figure 1a) is dominated by a single symmetric broad band peaking at 578.5 nm, which can be attributed to Eu(III) ions located in surface sites. The sample was in fact prepared by impregnating the surface of the ceria-zirconia powder with an Eu(III) solution. The mild heat treatment applied after the impregnation procedure cannot induce significant Eu(III) diffusion. On the other hand, the emission spectrum in the $^5D_0 \rightarrow {}^7F_0$ region for the high surface area bulk-doped CZE-20, prepared by coprecipitation, shows a broad asymmetric band located at 578.9 nm, likely a convolution of two bands, onto which another feature peaking at 580.5 nm is superimposed (Figure 1b). The band at longer wavelength can be associated to Eu(III) ions located in the bulk of the material and that at shorter wavelength with Eu(III) in surface sites, in agreement with the spectrum observed for the surface-doped sample (Figure 1a). We point out that the surface sites are likely to be more distorted than the bulk ones, and therefore they feature more prominently in the spectrum, even though they are presumably less abundant. Moreover, it is likely that the bulk sites are characterized by more covalent Eu−O bonds than the surface ones, and therefore their $^5D_0 \rightarrow {}^7F_0$ band is expected to be located at higher wavelength due to a stronger nephelauxetic effect.[22]

The spectrum of the bulk-doped CZE-20 treated at 1673 K (Figure 1d) also shows two bands (located at 579.5 and 580.5 nm) that, on the basis of the negligible surface area of this material, are attributed to bulk sites; however, the tetragonal structure cannot explain the presence of more than one site. The observed behavior can be interpreted assuming the presence of two distinct sites in the CZE-20 material, as observed in the literature using EXAFS, related respectively to cerium and zirconium ions.[29] In fact, the observation of distorted sites agrees with EXAFS results showing that Zr(IV) ions (cation radius: 0.072 nm) are located in distorted sites characterized by a coordination number lower than 8, the value found for the majority Ce(IV) ions (cation radius: 0.094 nm) located in O_h sites. We point out that the use of the Eu(III) ions (cation radius:

(28) Speghini, A.; Bettinelli, M.; Riello, P.; Bucella, S.; Benedetti, A. *J. Mater. Res.* **2005**, *20* (10), 2780–2791.

(29) Vlaic, G.; Fornasiero, P.; Geremia, S.; Kaspar, J.; Graziani, M. *J. Catal.* **1997**, *168* (2), 386–392.

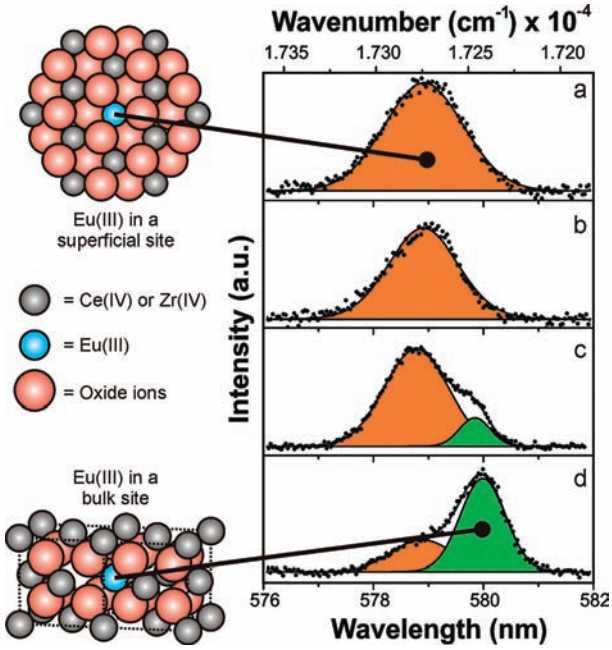

Figure 2. Eu(III) emission spectra of the thermodynamically stable cubic CZE-80 samples with the schematic representation of the Eu surface site located on the stable (111) surface of cubic $Ce_{0.8}Zr_{0.2}O_2$ and of the single Eu bulk site of $Ce_{0.8}Zr_{0.2}O_2$ as indicated by EXAFS data.[29] The details of the $^5D_0 \rightarrow {}^7F_0$ transition are reported for both surface and bulk Eu(III) doped materials after different thermal treatments: (a) surface-doped CZE-80 calcined at 773 K for 5 h, (b) surface-doped CZE-80 calcined at 1273 K for 5 h, (c) bulk-doped CZE-80 calcined at 773 K for 5 h, (d) bulk-doped CZE-80 calcined at 1273 K for 5 h. In accordance with XRD pattern and Raman spectra, all materials show Eu(III) emission spectra consistent with the presence of a single cubic *c* phase.

0.121 nm) as a structural probe gives detailed information about the local environment of the cations in these important materials. This information cannot be obtained by X-ray diffraction and/or Raman spectroscopy, as luminescence spectroscopy provides evidence for cationic inhomogeneity at the nanoscale level. In agreement with this assumption, all three contributions are observed in the region of the spectrum relative to the 0−0 transition for the bulk-doped CZE-20 treated at 1273 K (Figure 1c), which still possesses considerable surface area (Table 1).

The CZE-80 materials are cubic and the luminescence spectra are weak, due to the centrosymmetric nature of the crystallographic cationic sites (having O_h symmetry). The spectra resemble those reported for CeO_2:Eu(III),[30] dominated by the magnetic dipole $^5D_0 \rightarrow {}^7F_1$ transition. In O_h symmetry, the $^5D_0 \rightarrow {}^7F_0$ transition is forbidden[27] and therefore it is not observed for Eu(III) located in the regular cationic sites; however, weak features are observed in the 576−582 nm region (Figure 2). For the surface-doped CZE-80 samples (Figure 2, traces a and b), the emission spectra are similar to those previously observed for CZE-20: a single band centered at 578.9 nm is observed. It is important to highlight that the position of the band is not dependent on the thermal pretreatment subjected to the CZE-80 material. Moreover, it is only marginally affected by the crystal structure of the sample (cubic or tetragonal). In fact, the most stable surfaces—(111) surface for the cubic space group and (101) surface for the tetragonal space group—have similar structures, leading to similar geometries of the cationic site occupied by Eu(III).

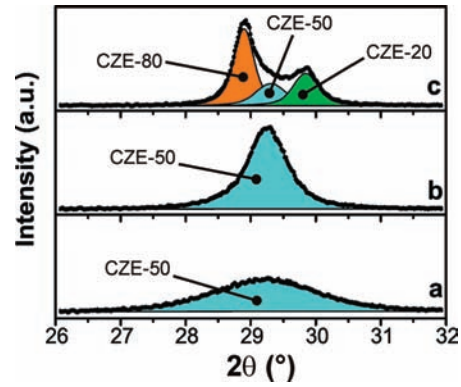

Figure 3. Detail of the normalized XRD patterns of CZE-50 after various thermal treatments showing the fitting of the main reflections. The presence of a single symmetric reflection for both the (a) bulk-doped CZE-50 calcined at 773 K for 5 h and (b) bulk-doped CZE-50 calcined at 1273 K for 2 h suggest the existence of a single phase CZE-50. In the case of (c) bulk-doped CZE-50 calcined at 1373 K for 20 h, the presence of at least 3 XRD reflections in the 26°−32° range clearly indicates the coexistence of the metastable CZE-50 material with one cerium- and one zirconium-reach phase.

In the case of bulk-doped CZE-80 calcined at 773 K (Figure 2c), the surface area is large and the band located at 578.5 nm is assigned to surface sites (see above). The weak shoulder around 580.0 nm can be related to minority bulk sites characterized by a noncentrosymmetric local structure. As the calcination temperature is increased to 1273 K, the surface area strongly decreases and the relative intensity of the two features at 578.5 and 580.0 nm (Figure 2d) clearly reverses, with the bulk Eu(III) becoming dominant in the luminescence spectrum.

Analysis of Metastable $Ce_xZr_{1-x}O_2$ Materials. $Ce_xZr_{1-x}O_2$ materials with intermediate composition are the most interesting for their catalytic applications, due to the higher capability to release and absorb oxygen (the so-called Oxygen Storage Capacity, OSC).[2,31,32] On the basis of the $Ce_xZr_{1-x}O_2$ phase diagram,[2,11,12] materials having composition $0.20 < x < 0.8$ are considered metastable. On the other hand, apparently single phase, "homogeneous" (on the XRD scale) materials were reported in the literature, depending on the synthetic method.[33−35] These materials could also be formed by domains (2−3 nm) with different compositions: this situation can be revealed only by complex and nonconventional techniques such as neutron diffraction.[19] As a significant example of metastable $Ce_xZr_{1-x}O_2$ material, samples with $x = 0.50$ were prepared and their structural, textural, and luminescence properties were analyzed after different thermal treatments.

The homogeneity of the CZE-50 sample, as a function of calcination temperature, was first checked by Rietveld analysis of the data obtained by conventional XRD. Figure 3 presents a detail of the XRD patterns in the region $2\theta = 26°-32°$. In this region, only one XRD reflection is present for the cubic (space group $Fm\bar{3}m$) and for the tetragonal (space group $P4_2nmc$) phases of $Ce_xZr_{1-x}O_2$. Therefore, it is commonly accepted that

(30) Fujihara, S.; Oikawa, M. *J. Appl. Phys.* **2004**, *95* (12), 8002–8006.
(31) Vidal, H.; Kaspar, J.; Pijolat, M.; Colon, G.; Bernal, S.; Cordon, A.; Perrichon, V.; Fally, F. *Appl. Catal., B* **2001**, *30* (1−2), 75–85.
(32) Vidal, H.; Kaspar, J.; Pijolat, M.; Colon, G.; Bernal, S.; Cordon, A.; Perrichon, V.; Fally, F. *Appl. Catal., B* **2000**, *27* (1), 49–63.
(33) Vlaic, G.; Di Monte, R.; Fornasiero, P.; Fonda, E.; Kaspar, J.; Graziani, M. *Stud. Surf. Sci. Catal.* **1998**, *116*, 185–195.
(34) Alifanti, M.; Baps, B.; Blangenois, N.; Naud, J.; Grange, P.; Delmon, B. *Chem. Mater.* **2003**, *15* (2), 395–403.
(35) Kaspar, J.; Fornasiero, P.; Balducci, G.; Di Monte, R.; Hickey, N.; Sergo, V. *Inorg. Chim. Acta* **2003**, *349*, 217–226.

Table 2. Physical Characteristics of the Thermodynamically Metastable CZE-50 Materials after Various Thermal Treatments

sample	treatment	BET surface area ($m^2\ g^{-1}$)	phase (wt%)	a [a] (nm)	c [a] (nm)	c/a	crystallite size[b] (nm)
bulk-doped CZE-50	773 K, 5 h	142	t'' ($P4_2nmc$) (100%)	0.5278	0.5286	1.001	5
	1273 K, 2 h	38	t'' ($P4_2nmc$) (100%)	0.5251	0.5292	1.008	13
	1373 K, 20 h	6	t' ($P4_2nmc$) (35%)	0.5145	0.5238	1.018	19
			t' ($P4_2nmc$) (38%)	0.5241	0.5323	1.016	14
			c ($Fm\bar{3}m$) (27%)	0.5344	---	1	28
surface-doped CZE-50	773 K, 5 h	125	t'' ($P4_2nmc$) (100%)	0.5284	0.5296	1.002	6
	1373 K, 20 h	3	t' ($P4_2nmc$) (47%)	0.5148	0.5241	1.018	26
			t' ($P4_2nmc$) (17%)	0.5260	0.5323	1.012	18
			c ($Fm\bar{3}m$) (36%)	0.5362	---	1	32

[a] Values for the pseudocubic unit cell. [b] Calculated applying the Scherrer formula to the (101) reflection of the tetragonal phase or to the (111) reflection of the cubic phase.

the number of peaks used to fit this part of the XRD pattern nicely correlates with the number of phases present in the sample. Table 2 summarizes the structural and textural properties of the CZE-50 samples involved in this study. Despite the metastable nature of this composition, after calcination at 773 K the material appears to be homogeneous on the XRD scale (only one peak is needed to fit the profile, Figure 3a) and is identified as in the t'' phase by Raman spectroscopy (see Supporting Information, Figure S8). While a partial sintering is observed, the CZE-50 material appears still homogeneous on the XRD scale after treatment at 1273 K (Figure 3b). Finally, in agreement with the metastable nature of this composition, prolonged aging at a higher temperature (1373 K) induces not only the complete collapse of the surface area but also a significant separation of phases (three peaks are recognized in the $2\theta = 26°-32°$ region, Figure 3c). Rietveld analysis of the XRD pattern of this sample (see Supporting Information, Figure S7 trace c′ and Table 2) reveals the presence of two t' phases (with cell parameters similar to those of the samples with $x = 0.20$ and 0.50) and a c phase (similar to the sample with $x = 0.80$). In agreement, also new bands appear in the Raman spectra of the CZE-50 material calcined at high temperature (see Supporting Information, Figure S8). The same considerations are valid also for the surface-doped samples (see Supporting Information, Figures S7 and S8).

The situation of the luminescence spectra of the CZE-50 materials is more complicated with respect to the ones of the thermally stable materials. A single band extending from 577.0 to 581.0 nm is observed in the case of the surface-doped CZE-50 sample, calcined at 773 K (Figure 4d). This is consistent with the Rietveld analysis of the XRD patterns that indicates the presence of a homogeneous, single phase material. On the contrary, the sample obtained by Eu surface impregnation on the CZE-50 sample previously calcined at 1373 K (Figure 4e) shows a feature completely different from all the spectra obtained from the impregnated single phase surface-doped samples (CZE-20 and CZE-80). In accordance with the XRD data, it can be related to phase inhomogeneity in the material.

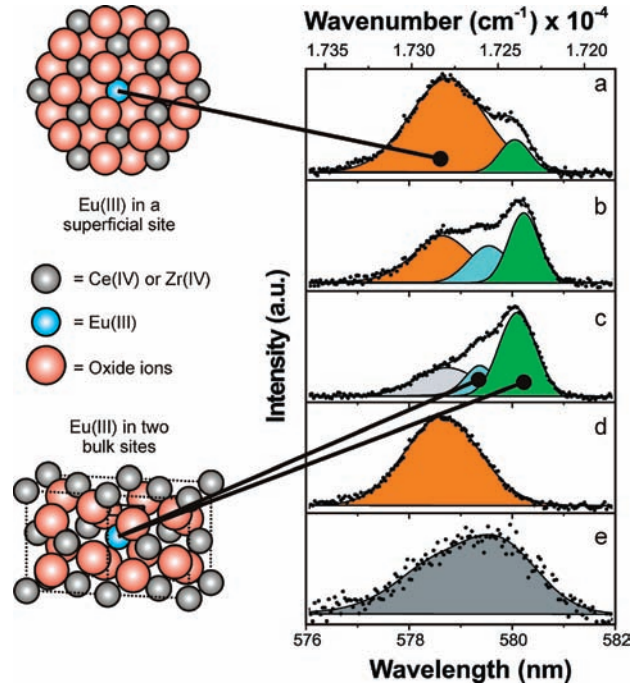

Figure 4. Eu(III) emission spectra of the thermodynamically metastable CZE-50 samples and schematic representation of the Eu surface site located on the stable (101) surface of the t'' phase of $Ce_{0.5}Zr_{0.5}O_2$ and of the two Eu bulk sites of $Ce_{0.5}Zr_{0.5}O_2$ as indicated by EXAFS data.[29] The details of the $^5D_0 \rightarrow {}^7F_0$ transition are reported for both surface and bulk Eu(III) doped materials after different thermal treatments: (a) bulk-doped CZE-50 calcined at 773 K for 5 h, (b) bulk-doped CZE-50 calcined at 1273 K for 2 h, (c) bulk-doped CZE-50 calcined at 1373 K for 20 h, (d) surface-doped CZE-50 calcined at 773 K for 5 h, (e) surface-doped CZE-50 previously calcined at 1373 K for 20 h. In accordance with XRD pattern and Raman spectra and phase diagram, high temperature calcination leads to phase separation.

In fact, a very broad convolution of various luminescence bands is observed in the wavelength range from 577.0 to 582.0 nm (Figure 4e).

In the case of the bulk-doped CZE-50 treated at 773 K, the spectrum (Figure 4a) shows two relatively broad bands peaking

at 578.6 and 580.0 nm, which can be assigned to Eu present on the surface and in bulk sites, respectively. This supports the XRD evidence that low temperature calcined bulk-doped CZE-50 material is a homogeneous material.

After severe calcination treatments (1273 and 1373 K), the intensity of the Eu on surface site band at ~578.5 nm progressively decreases, in agreement with the collapse of the surface area of the material (Table 2). The luminescence spectra of these two samples (Figure 4b and 4c) show a complex asymmetric structure extending from 578.0 to 581.0 nm. In the case of the very low surface area material treated at 1373 K, this feature must be essentially related to bulk sites. However, at least three different contributions, cationic sites, can be discriminated. The emission profile (Figure 4c) appears to be compatible with the overlapping of the bands at about 579.5 and 580.5 nm observed for the bulk-doped CZE-20 and at ~580.0 nm of the bulk- doped CZE-80. This observation is in agreement with the presence, in bulk-doped CZE-50 samples, of a deep phase separation (as evidenced by XRD), the Eu(III) probe ions being accommodated in sites typical of cubic and tetragonal phases. When the bulk-doped CZE-50 sample undergoes heat treatment at 1273 K, simulating aging in a TWC or in a SOFC, the two features mentioned above (578.6 and 580.0 nm) are still present (Figure 4b), but the relative intensity of the band assigned to surface sites decreases, due to the sharp decrease in the surface area (Table 2). Notably, the two features are not very distinguishable, and a third band starts to emerge around 579.3 nm. This situation is the result of the overlapping of the band related to the surface sites with two bands originating from the bulk, similarly to that previously observed for the tetragonal bulk-doped CZE-20. Notably, the bulk-doped CZE-50 can be classified as in the t'' phase, and the distortion of oxygen ions around the cationic sites is much less pronounced with respect to that in the t' phase of the bulk-doped CZE-20 and more similar to the oxygen coordination of the c phase of the bulk-doped CZE-80. Considering this, the two features at higher wavelengths cannot be ascribed to two different bulk sites on a homogeneous phase. These features are more likely to be related to Eu(III) distributed between phases with different compositions and oxygen geometries around the cationic sites, indicating that the sample could be formed by a mixture of domains with different compositions. Eu(III) luminescence can therefore evidence the inhomogeneity at the nanoscopic level, which is precluded using conventional characterization techniques, such as XRD or Raman spectroscopy.

Conclusions

Summarizing, we have prepared $Ce_xZr_{1-x}O_2$ mixed oxides doped with the Eu(III) ion, present in low amounts as a spectroscopic probe for the Ce(IV) and Zr(IV) sites, so that the chemical and physical properties of the materials are not significantly affected. Eu(III) luminescence spectroscopy of these materials can yield interesting and valuable information about the nature and thermal evolution of the cationic sites available to the probe ion and the phase inhomogeneity of the samples. As a general rule, for homogeneous materials a single, symmetrical band around 578.5 nm is obtained for Eu(III) deposited on the surface irrespective of the composition, crystal structure, and calcination treatment. In addition, luminescence spectra of the Eu(III) incorporated into the material during the sol−gel process provide structural information of the ceria-zirconia solid solution in the bulk. Remarkably, metastable $Ce_{0.5}Zr_{0.5}O_2$ materials, after aging at 1273 K to simulate use in TWCs or SOFCs, appear to be homogeneous to XRD and Raman analysis, but Eu(III) luminescence spectra indicate the presence of domains of different phases. This information is complementary to that obtained by sophisticated techniques, such as neutron diffraction and EXAFS.

Finally, high temperature redox treatments can induce migration of Eu ions from the surface to bulk opening new perspectives for in situ investigation of these materials.

Acknowledgment. The authors gratefully acknowledge the Universities of Trieste and Verona, ICCOM-CNR, INSTM, and PRIN2007 "Sustainable processes of 2nd generation for the production of H_2 from renewable resources", for financial support.

Supporting Information Available: XRD patterns of the investigated samples, including Rietveld analysis of the samples calcined at high temperature, Raman spectra and full luminescence spectra (range 570−725 nm). This material is available free of charge via the Internet at http://pubs.acs.org.

JA905158P